Am J Nucl Med Mol Imaging 2021;11(3):178-187
www.ajnmmi.us /ISSN:2160-8407/ajnmmi0131897

Original Article

SUV_{max} values at FDG PET-CT to predict malignancy in lymph nodes aspirated by real time image fused USgFNAC in head and neck squamous cell carcinoma

Petra K de Koekkoek-Doll[1], Wouter Vogel[2,3], Monique Maas[1], Jonas Castelijns[1], Laura Smit[4], Joannis Zavrakidis[5], Regina Beets-Tan[1], Michiel van den Brekel[6,7]

Departments of [1]Radiology, [2]Nuclear Medicine, [3]Radiation Oncology, [4]Pathology, [5]Epidemiology & Biostatistics, [6]Head and Neck Surgery & Oncology, The Netherlands Cancer Institute, Amsterdam, Netherlands; [7]Department of Maxillofacial Surgery, Amsterdam University Medical Center, Amsterdam, Netherlands

Received February 15, 2021; Accepted May 17, 2021; Epub June 15, 2021; Published June 30, 2021

Abstract: ^{18}F-fluordeoxyglucose (FDG) positron emission tomography combined with computed tomography (PET-CT) and ultrasound guided fine-needle aspiration cytology (USgFNAC) are commonly used to detect nodal metastases in head and neck squamous cell carcinoma (HNSCC). FDG PET-CT helps to guide selection of borderline suspicious nodes to aspirate using USgFNAC. Real time image fusion of FDG PET-CT with US is a new available technique and can improve this selection. The aim of this study was to determine optimal SUV_{max} values for USgFNAC node selection to improve USgFNAC sensitivity. 118 patients, with histopathological proven HNSCC or proven lymph nodes metastases of SCC of unknown primary, referred for staging of HNSCC with FDG PET-CT and ultrasound, were prospectively included. Additionally to standard USgFNAC of suspicious nodes fusion was performed to confirm that USgFNAC took place in FDG-positive nodes and to add Fused-USgFNAC in missed FDG-positive nodes. Fusion was performed on nodes with reported having metabolic activity. SUV_{max} values were measured in all Fused-USgFNAC nodes. The reference standard was cytology. In 118 patients USgFNAC was performed in 281 nodes. At fusion 22/281 (8%) nodes were FDG-negative. Out of 259 FDG-positive nodes 253 (98%) nodes were fused successfully. USgFNAC had conclusive results in 237/253 nodes (94%). In 126/237 nodes (53%) cytology proved to be tumor positive. Below SUV_{max} of 2.87 no fused FDG-positive nodes proved to be tumor positive at cytology. To improve sensitivity, only FDG-positive nodes with SUV_{max} values above 2.87 should be selected for USgFNAC. Image fusion can identify those nodes for USgFNAC selection.

Keywords: Head and neck cancer, lymph node metastasis staging, hybrid imaging, real-time image fusion, ultrasound FDG-PET, SUV_{max}

Introduction

The prognosis of head and neck squamous cell carcinoma (HNSSC) depends on many factors. Especially in HPV negative tumors the presence or absence of metastatic lymph nodes (N-stage) is one of the most important predictors for loco regional control and risk for distant metastasis and thereby highly influences the patient's management [1]. The number of metastases, their laterality, the involved node levels and the presence of extracapsular spread are important predictive parameters [2]. In a systematic review Lodder et al. reported that increasing volume of involved nodes is correlated with worsening outcome [3].

Management of cervical nodes often includes neck dissection (ND), radiotherapy (RT) or chemo-radiation (CRT). The extent of ND and RT as well as the dose of RT depend on the N-stage. Elective treatment is not always necessary if the risk of occult metastases is very low. To minimize treatment morbidity, accurate staging is thus very important [4, 5]. A systematic review and meta-analysis of elective neck dissection vs active surveillance of cT1-T2N0 squamous cell carcinoma (SCC) of the oral cavity showed that elective neck dissection (END) results in fewer regional recurrences than active surveillance [6]. Still, watchful waiting is considered a treatment option in case of a low risk for metastases and a very close follow-up of the neck [7].

For radiotherapy target volume selection and dose it is equally essential to know the N-status [8, 9]. Palpation of neck nodes is insufficient with a sensitivity and specificity in the range of 60-70% [10, 11]. The detection of malignant nodes by CT and MRI mainly relies on size criteria and has only a moderate sensitivity (74-78%) and specificity (76-80%) [12]. US-guided fine needle aspiration cytology (USgFNAC) has a very high specificity, but to obtain a high level of sensitivity many lymph nodes should be aspirated including nodes with a minimal axial diameter as small as 3-4 mm [13]. The challenge is to sample the right nodes to minimize false-negativity [14].

Precision medicine and molecular imaging technologies play a major rule in cancer diagnostic and therapy [15]. Molecular imaging with ^{18}F-fluordeoxyglucose positron emission tomography combined with computed tomography (FDG PET-CT) is increasingly used as a diagnostic tool to detect metastatic lymph nodes in the neck with a pooled sensitivity and specificity of 84% and 96%, respectively [16]. However, in patients with cT1-T2N0 oral cavity SCC sensitivity of FDG PET-CT drops to 50-58% [12, 17]. To increase the sensitivity a lower SUV uptake cut-off could be chosen, but then specificity drops unacceptably. FDG PET-CT frequently shows lymph nodes with visually borderline metabolic activity. These nodes are difficult to categorize as either malignant or reactive on PET-CT. Image fusion could help to identify and select nodes for Fused-USgFNAC which could help to increase specificity of PET-CT and sensitivity of USgFNAC.

We recently determined that real-time fusion of FDG PET-CT and ultrasound in Head and Neck Cancer (HNC) is technically feasible and allows FNAC-guidance by FDG uptake in lymph nodes (Fused-USgFNAC). In our study we found that 54% of the reported FDG-positive nodes could be proven as malignant at subsequent Fused-USgFNAC [18]. These data also suggested that small FDG-positive nodes can be detected with this technique, which enabled improved detection rate of malignant nodes. Based on these earlier results, the aim of this study is to establish a threshold of the SUV_{max} value to optimally select nodes to aspirate using USgFNAC.

Materials and methods

This study was approved by the Institutional Review Board (IRBd20-126). We prospectively included 118 patients with histopathological proven HNSCC or proven lymph nodes metastases of SCC of unknown primary.

All patients were referred for FDG PET-CT and USgFNAC for N-staging. Contrast enhanced CT of the neck or MRI was present. Next to the group analysis including all patients a subgroup analysis of patients with clinically node negative neck (cN0) and of patients with human papillomavirus (HPV) associated HHSCC was performed.

Data were analyzed retrospectively. All retrospective medical data/biospecimen studies at the Netherlands Cancer Institute have been executed pursuant to Dutch legislation and international standards. Prior to 25 May 2019, national legislation on data protection was applied, as well as the International Guideline on Good Clinical Practice. From 25 May 2019 we also adhere to the GDPR. Within this framework, patients are informed and have always had the opportunity to object or actively consent to the (continued) use of their personal data & biospecimens in research. None of the patients included in this study objected to use of their data.

FDG PET/CT imaging

FDG PET/CT images were acquired in the clinical setting using a Gemini TF scanner (Philips, Maryland, USA). Patients fasted for 6 hours and were hydrated prior to administration of FDG. Diabetes mellitus needed to be regulated adequately and the plasma glucose level was required to be < 10 mmol/l. A dose of 190-240 MBq was administered depending on BMI. FDG PET images of the head-neck area were acquired for 3 bed positions of 3 minutes each and were reconstructed to 2 mm isotropic voxels. Low dose CT was acquired for attenuation correction and anatomical orientation with 40 mAs and 2 mm slices. In addition, images of the neck-thighs were acquired. All FDG PET/CT images were assessed by dedicated nuclear medicine radiologists in the clinical setting; reports of these examinations were used for the current study.

Ultrasound and real time image fusion with FDG PET-CT

All US and FNAC procedures where performed by one radiologist with more than 10 years of

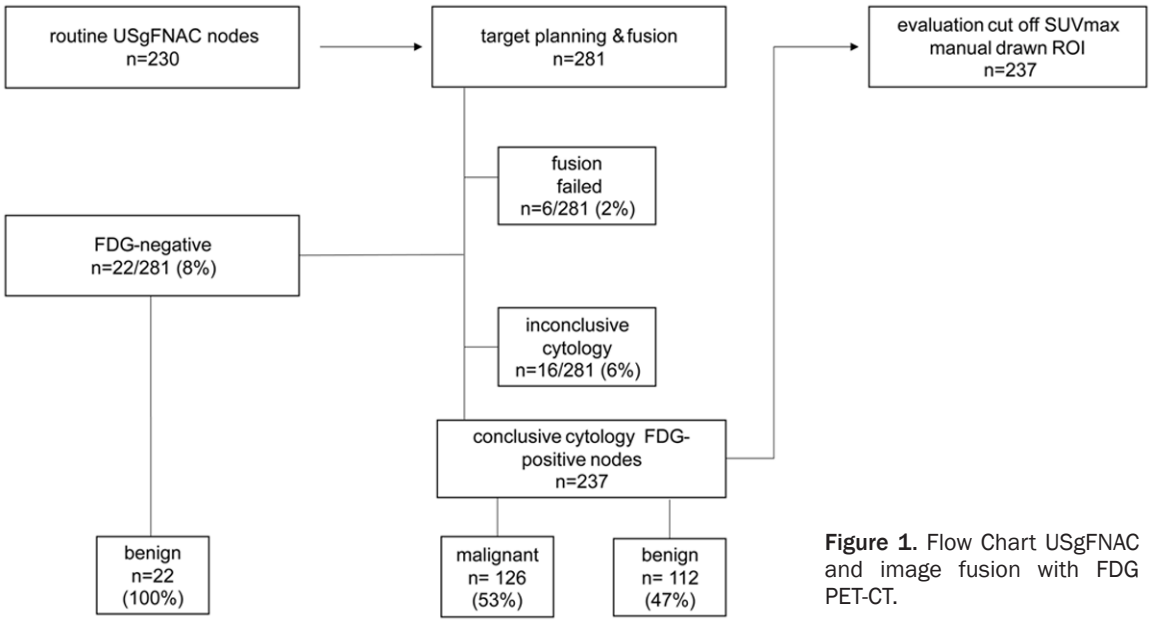

Figure 1. Flow Chart USgFNAC and image fusion with FDG PET-CT.

US experience in head and neck radiology (PDK). Ultrasound was performed by using an EpiQ7 G US device (Philips Medical Systems, Bothell, WA) with either an L12-5 or eL18-4 probe. A flow chart of the procedures is shown in **Figure 1**.

First, routine ultrasound of the ipsilateral and contralateral neck was performed. USgFNAC was performed in suspicious nodes according to Institutional guidelines. Criteria included loss of a fatty hilum, short axial diameter > 6-8 mm (depending on level), thickened or asymmetric cortex, round shape or suspicious nodes according to palpation or as seen on other imaging modalities (including CT, MRI or FDG PET/CT). Subsequently, ultrasound with real time image fusion with FDG PET-CT images was performed by the same radiologist (PKD), using the same US diagnostic system. The Percunav setup (Philips Medical Systems, Best, The Netherlands) was used according to the manufacturer's manual. For the L12-5 probe a bracket and an electromagnetic tracker were added. The eL18-4 probe has an integrated tracker. A patient reference tracker was placed on the forehead of the patient using tape. A field generator was fixed at a metallic arm positioned above the neck of the patient. FDG PET-CT data were imported into the US device and fusion of FDG PET and CT took place in the same device. An initial fusion between live US and FDG PET-CT was performed manually based on the thyroid gland, using the "match plane function". Additional manual corrections of the initial fusion were made, if necessary, by identification of known anatomical structures such as the hyoid bone, submandibular gland or carotid artery bifurcation. After the initial fusion, nodes that showed visible increased FDG uptake (compared to normal surrounding tissues) and that had been reported as suspicious, were selected for real time image fusion by using the "target planning function" (**Figure 2**).

Nodes that already underwent routine USgFNAC were evaluated again to determine if they corresponded to a FDG-positive node. Thereafter, fused-USgFNAC was performed in visually FDG-positive nodes if missed on routine USgFNAC (**Figure 2**). USgFNAC of FDG-positive nodes was performed in a maximum of 2 ipsilateral levels, in maximally 2 contralateral levels and in the lowest level of each side. For all nodes that received USgFNAC, the SUV_{max} values were measured by the radiologist who performed the US (PKD) using dyna-CAD by manual drawing of ROIs.

Pathology

The reference standard was cytological result from USgFNAC nodes. For aspiration of all nodes an 21 G needle was used. Part of the FNAC material was processed in smears, air dried and stained with Giemsa stain. Another

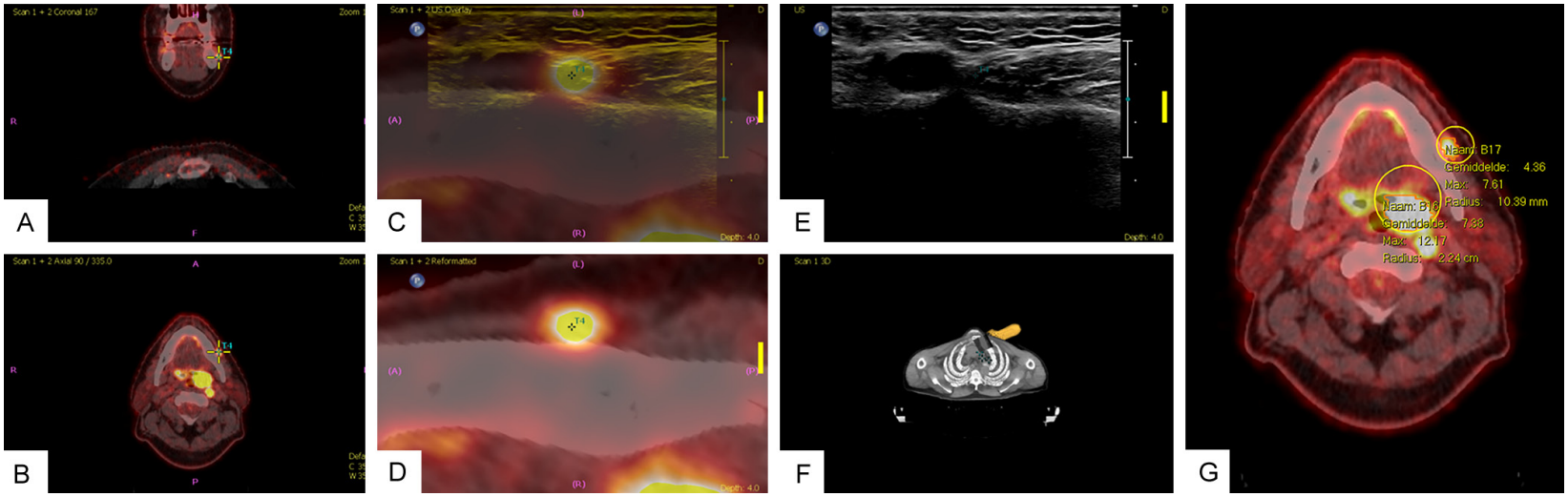

Figure 2. Target planning. fusion. and manual ROI placement of FDG-positive node to measure SUV_{max} values. A, B. Target planning PET- positive node 3D view. C. Real time fused PET-posive node, overlay US and PET-CT. D. Reformatted PET-CT image. E. US image. F. Volume representation of CT image and probe location. G. Manual drawing ROI in the Fused-USgFNAC node to measure SUV_{max} values.

Table 1. Diagnosis of all patients

Diagnose	n	%	HPV	HPV+	%	HPV-	%
SCC unkown primary	12	12.2%	12	6	50%	6	50%
SCC oral cavity	25	21.1%					
SCC oropharyngeal	33	28.0%	33	18	54%	15	46%
SCC hypopharyngeal	12	10.2%					
SCC laryngeal	23	19.5%					
SCC nasal cavity paranasal sinuses	6	5.1%	4	2	50%	2	50%
SCC nasopharyngeal	6	5.1%	4	2	50%	2	50%
SCC cutaneus	1	0.8%					
total	118	100%	53	28	53%	23	47%

part of every aspirate was fixed in 10 ml 4% formalin and embedded in paraffin for further immunohistochemistry if necessary, according to routine diagnostic workup. For clinically staging all samples were evaluated by experienced head and neck pathologists, the cytological results of the clinically setting were used retrospectively for the current study. HPV status was immunohistochemically assessed on formalin-fixed paraffin-embedded tissue samples from tumor biopsies or resections during standard routine diagnostic procedures. Antibodies for p53 (DO-7, 1/7000, DAKO) and p16 (E6H4; ready to use, Ventana Medical systems/Roche) were used in a Benchmark ULTRA autostainer (Ventane Medical systemsReactions were detected using OptiView DAB Detection kit (#760-700; Roche) for visualization p16 and p53. Finally, the slides were counterstained with Hematoxylin II and Bluing Reagent (Ventana Medical Systems).

Statistical evaluation

Calculation of sensitivity and specificity of the techniques was not possible as not all patients had a neck dissection with a pathology report. We therefore scored the percentage of positive cytology in relation to the SUV values in all nodes that were visually FDG-positive and aspirated at USgFNAC using image fusion. PET-negative nodes, nodes with failed fusion and nodes with inconclusive cytological results were excluded for further evaluation. Baseline characteristics were evaluated by descriptive statistics. A two-sided Independent samples t-test was used to compare the groups and subgroups and the two groups with positive and negative cytology based on their short axis diameter and SUV_{max}. A *p*-value of </= 0.05 was considered statistically significant.

Results

A total of 118 patients (median age of 63; range 32-89) with HNSCC were included. Diagnoses are shown in **Table 1**. In these 118 patients USgFNAC was performed in 281 nodes (**Figure 1**) Out of 281 nodes, 22 (8%) nodes were FDG-negative and all of these 22 nodes proved to be tumor negative at cytology. Image fusion failed in another 6 nodes (2%). Of the remaining 253 FDG-positive nodes, 16 (6%) had inconclusive cytological findings. These nodes were excluded from further evaluation. From the remaining, with image fusion confirmed 237 FDG-positive nodes, 126 (53%) had malignant cytology. The median size (diameter short axis) of all FDG-positive evaluated nodes was 10.3 mm (range 3-35 mm). The average size of nodes with malignant cytology was significantly larger than nodes with benign cytology, with a median size (diameter short axis) of 13.4 mm (range 4-35 mm) compared to 6.7 mm (range 3-15 mm), *p*-value < 0.0001. The mean SUV_{max} of all evaluated FDG-positive nodes was 7.8 (SD 5.8). The mean SUV_{max} in nodes with malignant cytology was also significant higher with an average 11.0 (SD 6.3) compared to benign nodes with an average 4.3 (SD 1.7), *p*-value < 0.0001 (**Table 2**). The lowest SUV_{max} in nodes with malignant cytology was 2.87 and the highest SUV_{max} in nodes with benign cytology was 10.7 (**Table 3**; **Figures 3**, **4**).

Subgroup analysis of clinically node negative neck (cN0) patients

Clinically 35/118 (30%) patients had a cN0 neck. In these patients, USgFNAC was performed in 71 FDG-positive nodes and 20 out of these (28%) had malignant cytology. The medi-

Table 2. Mean SUV_{max} and size (short-axis diameter) in FDG-positive nodes of all HNSCC patients

nodes	n	%	size			SUV_{max}		
			median	min	max	median	min	max
malignant	125	53%	13.4	4	35	11.0	2.87	40.84
benign	112	47%	6.7	3	15	4.3	1.95	10.7
all	237	100%	10.3	3	35	7.8	1.95	40.84

Table 3. SUV_{max} in ranges and number of malignant and benign nodes

SUV_{max}		nodes			benign		malignant	
>	≤	n	%	mean mm	n	%	n	%
	2	0	0%		0	0%	0	0%
2	2.5	5	2%	5.80	5	5%	0	0%
2.5	3	12	5%	6.42	11	10%	1	1%
3	3.5	29	12%	6.55	28	25%	1	1%
3.5	4	22	9%	6.14	17	15%	5	4%
4	4.5	20	8%	7.95	14	13%	6	5%
4.5	5	10	4%	6.80	8	7%	2	2%
5	5.5	17	7%	7.24	11	10%	6	5%
5.5	6	8	3%	7.00	3	3%	5	4%
6	6.5	6	3%	8.00	4	4%	2	2%
6.5	7	5	2%	8.20	2	2%	3	2%
7	7.5	6	3%	14.33	2	2%	4	3%
7.5	8	7	3%	9.29	1	1%	6	5%
8	8.5	5	2%	14.40	0	0%	5	4%
8.5	9	10	4%	13.90	0	0%	10	8%
9	9.5	7	3%	10.57	0	0%	7	6%
9.5	10	10	4%	13.00	2	2%	8	6%
10	10.5	3	1%	13.00	1	1%	2	2%
10.5	11	8	3%	12.50	2	2%	6	5%
11	11.5	4	2%	15.75	0	0%	4	3%
11.5	12	4	2%	11.75	0	0%	4	3%
12	12.5	3	1%	16.67	0	0%	3	2%
12.5	13	4	2%	16.00	0	0%	4	3%
13	13.5	1	0%	16.00	0	0%	1	1%
13.5	14	2	1%	15.50	0	0%	2	2%
14	14.5	3	1%	14.67	0	0%	3	2%
14.5	15	2	1%	9.50	0	0%	2	2%
15		24	10%	19.63	0	0%	24	19%

an short axis of nodes in cN0 was significantly smaller, *p*-value 0.001 (7.8 mm, range 3-23) than in cN+ (10.6 mm, range 3-35). The median short axis of malignant cN0 nodes (10.1 range 4-23) was significant smaller, value 0.039 than in cN+ nodes (13.5, range 4-35). The mean SUV_{max} of cN0 nodes with malignant cytology was significantly higher than in nodes with benign cytology, with an average of 8.3 (SD 5.0) versus 4.45 (SD 1.8), *p* value < 0.003.

The mean SUV_{max} of malignant nodes in all cN+ necks was 13.5 (SD 7.2) while it was 8.3 (SD 5.0) in cN0 necks, which was significantly lower, *p*-value 0.002. The lowest SUV_{max} in nodes with malignant cytology was 3.6 and the highest SUV_{max} in nodes with benign cytology was 10.6.

Subgroup cut-off SUV_{max} values in HPV associated SSC of the oropharynx, nasopharynx and unknown primary

Immunohistochemically results of HPV related tumors were present in 53 patients.

In 28/53 patients the tumor was associated with HPV (HPV+) and USgFNAC was performed in 73 nodes. 48/73 nodes were malignant at cytology. Mean short axis was 13.8 mm (SD 7.1) and mean SUV_{max} was 9.6 (SD 4.8). 25/78 nodes were benign at cytology. Mean short axis was 7.2 mm (SD 1.99) and mean SUV_{max} was 4.96 (SD 1.99). The lowest SUV_{max} in nodes with malignant cytology was 3.39 and the highest SUV_{max} in nodes with benign cytology was 10.27.

In 25/53 patients the tumor was HPV negative (HPV-) and USgFNAC was performed in 45 nodes. 26/45 nodes were malignant at cytology. Mean short axis was 12.2 mm (SD 7.2), mean SUV_{max} was 10.9 (SD 5.1). 19/45 nodes were benign at cytology. Mean short axis was 7.4 mm (SD 2.2), mean SUV_{max} was 4.2 (SD 2.0).

The lowest SUV_{max} in nodes with malignant cytology was 2.87 and the highest SUV_{max} in

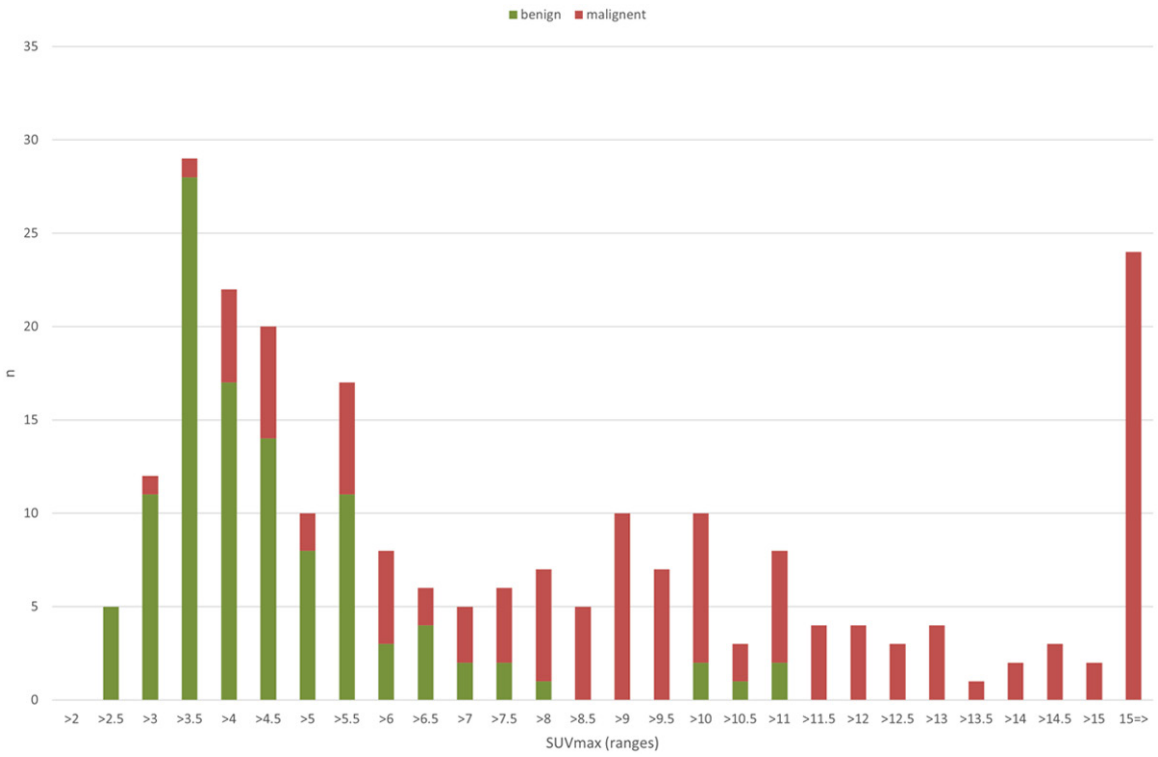

Figure 3. Suv_{max} ranges, n benign and malignant nodes.

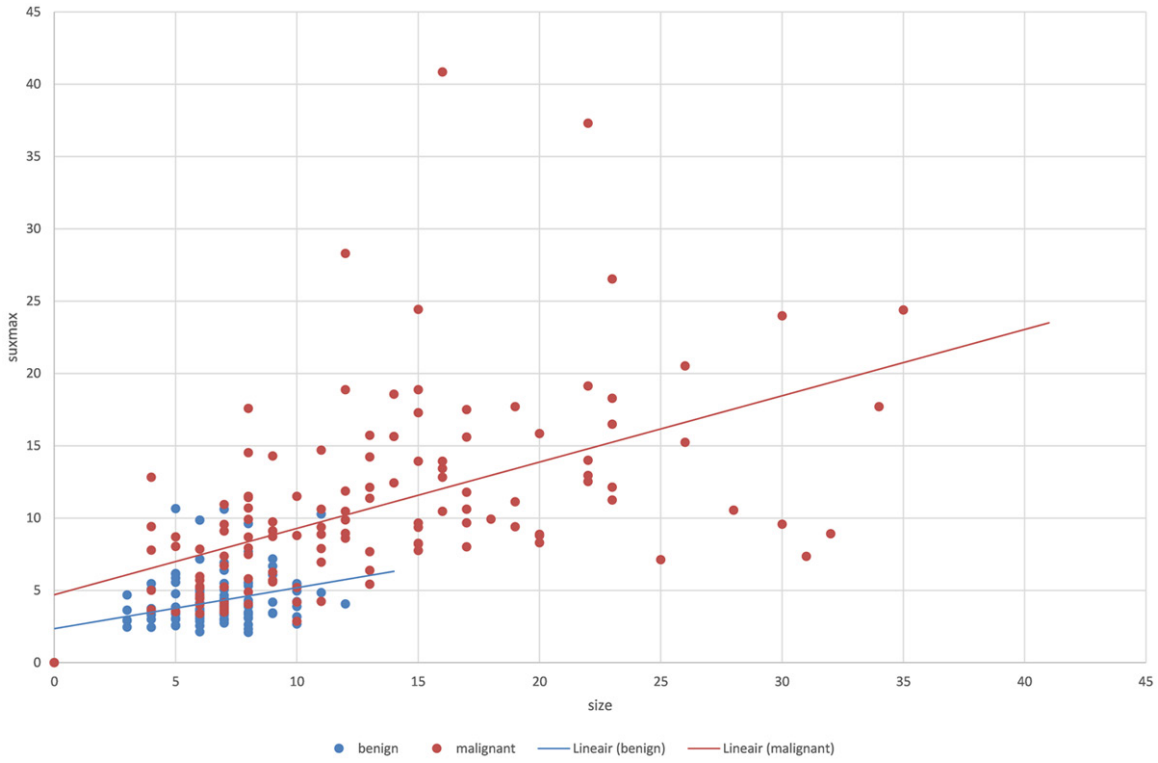

Figure 4. Scatterplot malignant and benign nodes, SUV_{max} and size.

nodes with benign cytology was 10.6. Mean SUV_{max} in malignant HPV- nodes was 10.6 and in malignant HPV+ nodes 9.6, statistically not significant *p* value = 0.279.

Discussion

The presence of cervical lymph node metastases in HNSCC has a large impact on patients prognosis and treatment [19, 20]. To detect occult nodal metastases in clinically node negative neck FDG PET-CT is slightly superior to MRI, CT or ultrasound [16, 21]. On the other hand, however, regarding the detection of cervical lymph node metastases in cN0 HNSCC patients, a recent meta-analysis still showed a low sensitivity and moderate specificity of FDG PET-CT [17]. This can be explained by the non-specific nature of FDG uptake in small nodes and the difficulty to distinguish between benign, reactive or inflammatory on the one hand and malignant nodes other hand. Although ultrasound enables detection of enlarged nodes and enables evaluation of additional morphological features of nodes, it does not enable detection of micro-metastases in small nodes [22]. In our study only 22/281 nodes which underwent USgFNAC where FDG-negative, none of these nodes proved to be malignant. On ultrasound it might be difficult to identify tiny FDG-positive nodes with regular morphology and the major challenge performing USgFNAC is to select the right tiny FDG-positive node to puncture (based on imaging features on US but also other modalities), whereas the major issue in FDG PET-CT is, how borderline SUV values should be interpreted. Generally, a node with a SUV_{max} value above 4.5 is considered to be metastatic, whereas the nature of nodes with a SUV-value below this value remains uncertain [23].

In our study malignant FDG-positive nodes in cN0 HNSCC patients were significantly smaller than in cN+ HNSCC patients and had a significant lower mean SUV_{max} value.

These small nodes are the nodes that are difficult to accurately select for aspiration with routine US. Due to image fusion we were able to localize small FDG-positive nodes with a normal morphological appearance on ultrasound to perform fused-USgFNAC. Out of the real time image fused guided FDG-positive FNAC nodes 53% proved to be malignant at cytology. Based on Fused USgFNAC none of the FDG-positive nodes with a SUV_{max} of </= 2.87 was malignant. Our data are comparable to a recent study in which comparing PET-CT-data with cytological results, below a SUV_{max} of 2.2 no malignant nodes were found [24]. Therefore, a threshold SUV_{max} > 2.87 can be used to guide US-FNAC. Using this value to select nodes for fused-USgFNAC will likely increase the accuracy of detection of malignant nodes in staging of HNSCC.

Based on Fused-USgFNAC at a SUV_{max} of 10.7 or higher all FDG-PET positive nodes were malignant and in fact in these nodes, aspiration might not be needed. A SUV_{max} value between 2.87 and 4.5 poses the major clinical problem, and in these cases, but also up to SUV_{max} 10.7 fused USgFNAC might be helpful to make the diagnosis.

Our results are also comparable with those in a study of Payabvash et al. who reported that at a $SUV_{max} \geq 2.5$ sensitivity for detection of malignant nodes was 100%, with histopathological results as reference standard [25]. Other studies that correlated with histology found higher cut-offs for SUV_{max} values for malignant nodes. Dequanter et al. compared FDG-PET-CT with histology after neck dissection and proposed a SUV_{max} cut-off-value of 4.05 to detect malignant nodes [26]. Using this cut-off-value in the current study 13 malignant nodes would have been missed. Because accurate N-stage is essential for treatment planning, a lower cut-off SUV_{max}, like >/= 2.87, is preferred to guide Fused-USgFNAC. To minimalize false negative results because of sampling errors, USgFNAC should be repeated in nodes with benign cytological results and a SUV_{max} of >/= 2.87, if relevant for treatment decision.

SUV_{max} values are reported significantly higher in HPV-negative nodes than in HPV-positive nodes [27]. In a meta-analysis of Fleming et al, a higher SUV_{max} value in HPV-negative tumors was found but PET SUV_{max} scores were unable to reliable differentiate between HPV-positive and HPV-negative tumors [28]. These results are comparable to our results with a statistically not significant higher mean SUV_{max} value in malignant HPV-negative nodes than in malignant HPV-positive nodes.

Limitations

Because all Fused-USgFNAC and measurements were performed by one radiologist, the interobserver variability of the procedure is unknown.

In this study histopathological results of neck dissection as a gold standard are not available; therefore sampling error, leading to false negative results of cytology cannot be excluded.

Conclusion

To improve the sensitivity, for FDG-positive nodes with a benign morphological appearance on ultrasound, a SUV_{max} value ≥ 2.87 should be used to select nodes for USgFNAC. Those FDG-positive nodes can be identified by real time image fusion and Fused-USgFNAC can be performed.

Acknowledgements

The authors would like to acknowledge Pedro Sanches, PhD and Frans Gleuwink (Philips Benelux, Boschdijk 525, 5621JG Eindhoven) for providing knowledge and training on Percunav image fusion (MR, CT, PET).

Disclosure of conflict of interest

None.

Address correspondence to: Dr. Petra K de Koekkoek-Doll, Department of Radiology, The Netherlands Cancer Institute, Plesmanlaan 121, 1066 CX, Amsterdam, The Netherlands. Tel: +31 20 5122003; E-mail: p.doll@nki.nl

References

[1] Godény M. Prognostic factors in advanced pharyngeal and oral cavity cancer; Significance of multimodality imaging in terms of 7th edition of TNM. Cancer Imaging 2014; 14: 1-13.

[2] Woolgar JA. Histopathological prognosticators in oral and oropharyngeal squamous cell carcinoma. Oral Oncol 2006; 42: 229-239.

[3] Lodder WL, Pameijer FA, Rasch CR, van den Brekel MW and Balm AJ. Prognostic significance of radiologically determined neck node volume: a systematic review. Oral Oncol 2012; 48: 298-302.

[4] Al-Mamgani A, Verheij M and van den Brekel MWM. Elective unilateral nodal irradiation in head and neck squamous cell carcinoma: a paradigm shift. Eur J Cancer 2017; 82: 1-5.

[5] Nieuwenhuis EJ, Castelijns JA, Pijpers R, van den Brekel MW, Brakenhoff RH, van der Waal I, Snow GB and Leemans CR. Wait-and-see policy for the N0 neck in early-stage oral and oropharyngeal squamous cell carcinoma using ultrasonography-guided cytology: is there a role for identification of the sentinel node? Head Neck 2002; 24: 282-9.

[6] Abu-Ghanem S, Yehuda M, Carmel NN, Leshno M, Abergel A, Gutfeld O and Fliss DM. Elective neck dissection vs observation in early-stage squamous cell carcinoma of the oral tongue with no clinically apparent lymph node metastasis in the neck. JAMA Otolaryngol Neck Surg 2016; 142: 857.

[7] Koyama LKS, Matos LL, Kulcsar MAV, de Araújo Filho VJF and Cernea CR. Oral cancer treatment: still an indication for elective neck dissection? ORL 2018; 80: 96-102.

[8] van den Bosch S, Vogel WV, Raaijmakers CP, Dijkema T, Terhaard CHJ, Al-Mamgani A and Kaanders JHAM. Implications of improved diagnostic imaging of small nodal metastases in head and neck cancer: radiotherapy target volume transformation and dose de-escalation. Radiother Oncol 2018; 128: 472-478.

[9] Navran A, Heemsbergen W, Janssen T, Hamming-Vrieze O, Jonker M, Zuur C, Verheij M, Remeijer P, Sonke JJ, van den Brekel M and Al-Mamgani A. The impact of margin reduction on outcome and toxicity in head and neck cancer patients treated with image-guided volumetric modulated arc therapy (VMAT). Radiother Oncol 2019; 130: 25-31.

[10] van den Brekel MW, Castelijns JA, Stel HV, van der Waal I, Tiwari RM and Snow GB. Diagnostiek van lymfekliermetastasen van hoofd-halscarcinomen. Ned Tijdschr Geneeskd 1995; 139: 1075-8.

[11] Geetha NT, Hallur N, Goudar G, Sikkerimath BC and Gudi SS. Cervical lymph node metastasis in oral squamous carcinoma preoperative assessment and histopathology after neck dissection. J Maxillofac Oral Surg 2010; 9: 42-7.

[12] Kyzas PA, Evangelou E, Denaxa-Kyza D and Ioannidis JP. 18F-fluorodeoxyglucose positron emission tomography to evaluate cervical node metastases in patients with head and neck squamous cell carcinoma: a meta-analysis. J Natl Cancer Inst 2008; 100: 712-720.

[13] van den Brekel MW and Castelijns JA. What the clinician wants to know: surgical perspective and ultrasound for lymph node imaging of the neck. Cancer Imaging 2005; 5 Spec No: 0-16.

[14] Borgemeester MC, van den Brekel MW, van Tinteren H, Smeele LE, Pameijer FA, van Velthuysen ML and Balm AJ. Ultrasound-guid-

ed aspiration cytology for the assessment of the clinically N0 neck: factors influencing its accuracy. Head Neck 2008; 30: 1505-1513.
[15] Ghasemi M, Nabipour I, Omrani A, Alipour Z and Assadi M. Precision medicine and molecular imaging: new targeted approaches toward cancer therapeutic and diagnosis. Am J Nucl Med Mol Imaging 2016; 6: 310-327.
[16] Sun R, Tang X, Yang Y and Zhang C. (18)FDG-PET/CT for the detection of regional nodal metastasis in patients with head and neck cancer: a meta-analysis. Oral Oncol 2015; 51: 314-20.
[17] Kim SJ, Pak K and Kim K. Diagnostic accuracy of F-18 FDG PET or PET/CT for detection of lymph node metastasis in clinically node negative head and neck cancer patients; A systematic review and meta-analysis. Am J Otolaryngol 2019; 40: 297-305.
[18] de Koekkoek-Doll PK, Maas M, Vogel W, Castelijns J, Smit L, Zavrakidis I, Beets-Tan R and van den Brekel M. Real-time ultrasound image fusion with FDG-PET/CT to perform fused image-guided fine-needle aspiration in neck nodes: feasibility and diagnostic value. AJNR Am J Neuroradiol 2021; 42: 566-572.
[19] Snow GB, Annyas AA, van Slooten EA, Bartelink H and Hart AA. Prognostic factors of neck node metastasis. Clin Otolaryngol Allied Sci 1982; 7: 185-92.
[20] Leemans CR, Tiwari R, Nauta JJ, van der Waal I and Snow GB. Regional lymph node involvement and its significance in the development of distant metastases in head and neck carcinoma. Cancer 1993; 71: 452-6.
[21] Yoon DY, Hwang HS, Chang SK, Rho YS, Ahn HY, Kim JH and Lee IJ. CT, MR, US, 18F-FDG PET/CT, and their combined use for the assessment of cervical lymph node metastases in squamous cell carcinoma of the head and neck. Eur Radiol 2009; 19: 634-642.
[22] Richards PS and Peacock TE. The role of ultrasound in the detection of cervical lymph node metastases in clinically NO squamous cell carcinoma of the head and neck. Cancer Imaging 2007; 7: 167-178.
[23] Lim RSM, Ramdave S, Beech P, Billah B, Karim MN, Smith JA, Safdar A and Sigston E. Utility of SUV_{max} on 18 F-FDG PET in detecting cervical nodal metastases. Cancer Imaging 2016; 16: 1-8.
[24] Peltenburg B, de Keizer B, Willem Dankbaar J, de Boer M, Willems SM, P Philippens ME, J Terhaard CH and de Bree R. Acta Oncologica Prediction of ultrasound guided fine needle aspiration cytology results by FDG PET-CT for lymph node metastases in head and neck squamous cell carcinoma patients Prediction of ultrasound guided fine needle aspiration cytology results by FDG PET-CT for lymph node metastases in head and neck squamous cell carcinoma patients. Acta Oncol 2018; 57: 1687-1692.
[25] Payabvash S, Meric K and Cayci Z. Differentiation of benign from malignant cervical lymph nodes in patients with head and neck cancer using PET/CT imaging. Clin Imaging 2016; 40: 101-105.
[26] Dequanter D, Shahla M, Aubert C, Deniz Y and Lothaire P. Prognostic value of FDG PET/CT in head and neck squamous cell carcinomas. Onco Targets Ther 2015; 8: 2279-2283.
[27] Tahari AK, Alluri K, Quon H, Koch W, Wahl RL, Subramaniam RM, Subramaniam R and Morgan RH. FDG PET/CT imaging of Oropharyngeal SCC: characteristics of HPV positive and negative tumors. Clin Nucl Med 2014; 39: 225-231.
[28] Fleming JC, Woo J, Moutasim K, Mellone M, Frampton SJ, Mead A, Ahmed W, Wood O, Robinson H, Ward M, Woelk CH, Ottensmeier CH, King E, Kim D, Blaydes JP and Thomas GJ. HPV, tumour metabolism and novel target identification in head and neck squamous cell carcinoma. Br J Cancer 2019; 120: 356-367.